



Robust dynamic fuzzy-based enhanced VPD/FQB controller for load sharing in microgrid with distributed generators

Subhashree Choudhury¹ · Pritam Bhowmik¹ · Pravat Kumar Rout¹

Received: 20 May 2017 / Accepted: 17 July 2018 / Published online: 26 July 2018
© Springer-Verlag GmbH Germany, part of Springer Nature 2018

Abstract

Microgrid control strategies are mostly accompanied by droop control to ensure voltage and frequency stability, and proportionate power sharing among distributed generation systems. However, conventional droop control may cause undesirable voltage and frequency deviations due to impedance mismatch of the DG feeders, different ratings of the DG units, and complex configurations (loop or mesh networks). To circumvent the above issue, it is necessary to design a dynamic approach for an improved power sharing without sacrificing any voltage and frequency deviations with optimum regulation and stability. In this paper, three conventional drooping topologies, namely as real power and reactive power drooping (PQ drooping), virtual impedance drooping, and voltage real power drooping or frequency reactive power boosting (VPD/FQB), are deployed and compared to investigate their efficiency and stability in the power sharing issues in low-voltage islanded microgrid system. Based on the simulated results, it has been observed that the conventional VPD/FQB topology is superior in load sharing over the other two topologies. However, the conventional VPD/FQB offers certain drawbacks in steady-state and dynamic stability under nonlinear and unsymmetrical load conditions. For further enhancement of the conventional VPD/FQB topology, a novel dynamic fuzzy logic controller (DFLC) is proposed in this study. Simulation results from the IEEE test system in MATLAB environment validate the performance of the proposed DFCLC-based VPD/FQB scheme under different operating conditions as compared to conventional VPD/FQB approach.

Keywords Distributed generation (DG) · Droop control · Virtual impedance · DC–AC power converters · Real and reactive power sharing · Dynamic fuzzy logic controller (DFLC)

1 Introduction

Conventional power system technologies face hard to deal with consistency in operation and control to the increased power demand and reliability requirement due to the rapid expansion of power grid network. As a result, to find the solution for the above issue in the last few years, new resolutions such as distributed generation (DG), microgrid, active demand management (ADM), and electrical energy storage (EES) have emerged as future works to accomplish. DG integration to the distribution sector is a promising effort in this direction to cope up with these problems. However, the involvement of DG poses many technical constraints such as the frequency stability, voltage stability, and the load sharing

etc. Despite few technical constraints arisen by DG coordination, it has few positive aspects to support the overall system performance like flexibility in installation, low-power transmission loss, reactive power support, and higher-energy utilization rate. Apart from that, the DG unit also gives the higher degree of controllability, thus allowing microgrid to play a major and critical role in maintaining the stability and reliability of electrical networks [1, 2]. So, an effective design and planning of smart distribution network in the smart grid environment can effectively get rid of the potential adverse impacts occurred due to DG integration related to control, protection and power quality. In case of an autonomous microgrid, all the DGs are equally responsible according to their rating to maintain the system voltage and frequency through optimally sharing the active and reactive power [3, 4]. To address the problem of load sharing without communication between the converters, an attempt has been made in this study to meet the electrical energy demand in the islanded mode of operation.

✉ Subhashree Choudhury
subhashree3@gmail.com

¹ Department of EEE, Siksha ‘O’ Anusandhan University, Bhubaneswar, India

Conventional droop control methods fail to perform optimally sharing of nonlinear loads due to the integrated control units to account simultaneously not only harmonic currents but also to regulate the active and reactive power in the distribution feeders. Due to not having large X/R ratio, the active and reactive power is highly coupled and dependent on voltage magnitude and phase angle. Further, the power sharing based on the droop method is affected by the output impedance of the units as well as the line impedance. Besides, the major limitations that lie in case of droop method are its load-dependent frequency and amplitude deviations. The dynamic response of an inertial DG is different from that of a non-inertial DG, and due to that, the mismatch in response rate can create the power and frequency fluctuations. In a nutshell, there is a need of further study on droop control approach application to the distribution system to focus on the issues like frequency and voltage deviations, harmonics loads, the different and unknown line impedances, and fluctuant and changeable output power of DGs. To overcome these limitations and to minimize the corresponding circulating current under all types of real-time conditions, various authors have proposed several modified droop control methods. All these methods can be categorized into four sections as: (1) conventional and variants of droop control; (2) virtual structure-based methods; (3) construct and compensate-based methods; and (4) hybrid droop/signal injection-based methods [5, 6]. This study is an attempt in this direction to enhance the performance of power sharing to circumvent the above issues fully/partly.

There have been several studies aimed at developing droop control to ensure voltage and frequency stability, and proportionate power sharing among distributed generation systems. Through appropriate droop control, the interfacing inverters can be directed to share proper loads operating in parallel as per the ratio of their individual ratings, without implementation of any communication line between them [7]. But, the precise power sharing in islanding mode through drooping methods is technically challenged by line impedances [8]. Hence, drooping schemes are to be chosen depending on the type of line or feeder impedances. In the recent past, three conventional drooping schemes for low-voltage microgrid operating in islanding mode, namely real and reactive power drooping (PQ drooping) [9, 10], virtual impedance drooping (VID) [11–13], and voltage real power drooping or frequency reactive power boosting (VPD/FQB) [14], have been proposed in the literature. However, VPD/FQB has major advantages over PQ drooping and VID technology in terms of improved power sharing and system stability for low-voltage microgrid [13, 14]. Also, it does not get affected by the physical parameters [15, 16].

The artificial intelligence methods such as artificial neural networks, fuzzy logic algorithm, evolutionary or genetic

algorithms, and expert systems are proficiently applied for various engineering applications. In particular to real-time online applications, neural network and evolutionary algorithm fails to meet the requirement due to large computational time involved. However, those techniques may have slightly edge over fuzzy logic for other offline applications. Secondly, particular to control application, fuzzy logic has the operational advantages like higher robustness, customizable, easily emulate human deductive thinking, higher reliability, and efficiency. Thirdly, it has been found with recently published article in the direction of load sharing in microgrid with distributed generation that fuzzy logic comparatively arrives at better solution with proper parameter setting either hybridizing with other controllers [17]. Looking to the above findings, these factors motivate us to use fuzzy logic even though varieties of artificial intelligent techniques are available in the literature [18]. As a nutshell, on the basis of practical implementation feasibility, we proceed to design the controller based on fuzzy logic. Generally, in present power network, PI controllers are more proficiently used. This present study is an attempt to design robust controller incorporation with both fuzzy logic and PI controllers to enhance the droop control performance based on VPD/FQB.

Communication-based power sharing techniques based on proportional–derivative (PD) and proportional–integral (PI) have been proposed and are found to be very sensitive to the operating conditions such as unpredictable load and the line parameters [19]. However, these controllers need to be tuned offline with the change of load or system parameters to enhance its robustness. To circumvent this associated problem in the PD/PI controller, various types of controllers based on fuzzy logic control (FLC) are proposed to handle the uncertainty and random variation of system parameters and loads. Even though controllers based on FLC outperform PD/PI-based controller by widening the robustness and performance, FLC is not completely independent of the values of fuzzy parameters. In this paper, to extract the advantages of both the aforesaid controllers, fuzzy input parameters are dynamically tuned by PI controller and by so the concept of constant fuzzy parameters is avoided. The proposed dynamic FLC (DFLC) performs robustly because like FLC it does not directly depend on error and change in error, but according to the requirement error is tuned through PI controller.

The salient features of the proposed controller this work focuses on are:

1. Dynamically changing the inputs of the FLC through PI controller to share the load demand among multiple parallel-connected inverters proportionately and to maintain the voltage and frequency stabilities.
2. Extensively study the dynamic stability of the test system and performance of the proposed approach subjected to variations in load, real, and reactive power.

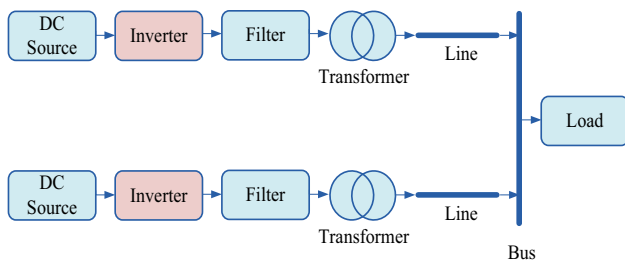


Fig. 1 Islanded connection scheme

3. Optimally computing the modulation index and to regulate the corresponding frequency for the VSIs based on simple SPWM technique.
4. To evaluate and verify the THD calculation through FFT analysis of power signals to be well within the IEEE prescribed limits.
5. To perform and present a detailed comparison between three conventional approaches and proposed DFLL technique based on VPD/FQB.

The rest part of the paper is organized as follows. Section 2 presents the system configuration in islanding mode and the corresponding mathematical modelling. The concept of drooping and the control strategies for conventional PQ drooping, VID, and VPD/FQB are described in Sect. 3. Section 4 illustrates the comparison among the aforesaid conventional drooping schemes. Description and detail modelling of the proposed scheme is illustrated in Sect. 5. In Sect. 6, simulation results and comparative analysis are enumerated. Finally, the conclusions from the entire study are drawn in Sect. 7.

2 System configuration in Islanded mode

Figure 1 illustrates the block diagram of an islanded microgrid which comprises of two parallel DG systems. Each DG system is integrated with voltage source inverter (VSI), LC filters, and step-down transformer. The parameters of the system are presented in “Appendix”.

3 Concept of drooping

The load sharing strategies work without inter-unit communication are generally based on droop concept and very often used for the control scheme of inverters located in remote areas. As compared to communication-based design, in droop control case the complexity of the controller design is less with improved reliability and redundancy during operation. In addition to that, droop control scheme has plug-and-play characteristics and so that a single unit of a module can be replaced without stopping the whole system function. There are various droop control strategies cited in the literature [20, 21].

4 Comparison of the conventional PQ, VID, and VPD/FQB schemes

Figure 2 shows the injected real and reactive power of inverter-1 subjected to the constant load. Figure 2a illustrates the real power delivered by the inverter-1 in case of the aforesaid three drooping topologies. Peak overshoots of the real power are 230.9 and 213.4 KW for the VPD/FQB and conventional VID, respectively. The rise time of the real power is 0.036 s for the conventional VPD/FQB as com-

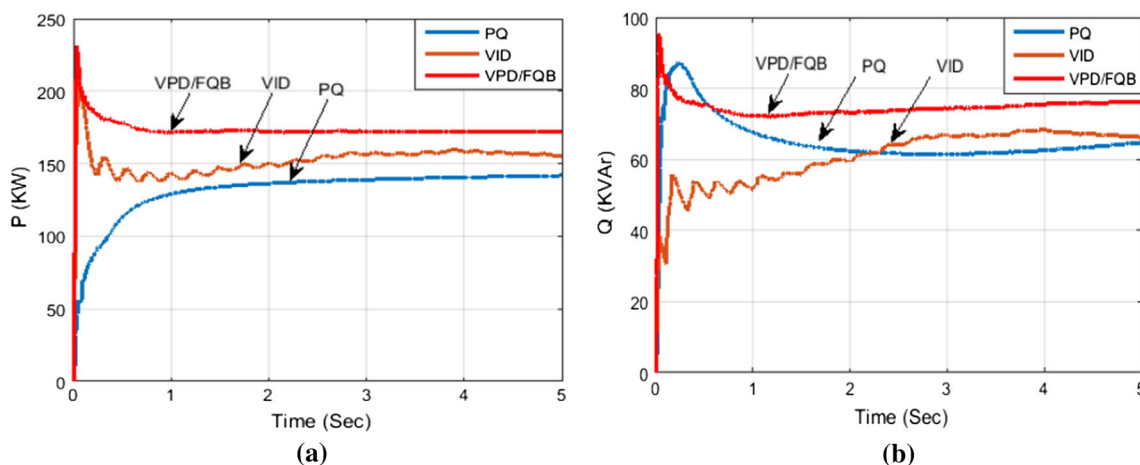


Fig. 2 a Real power injection by inverter-1 and b reactive power by injection by inverter-1

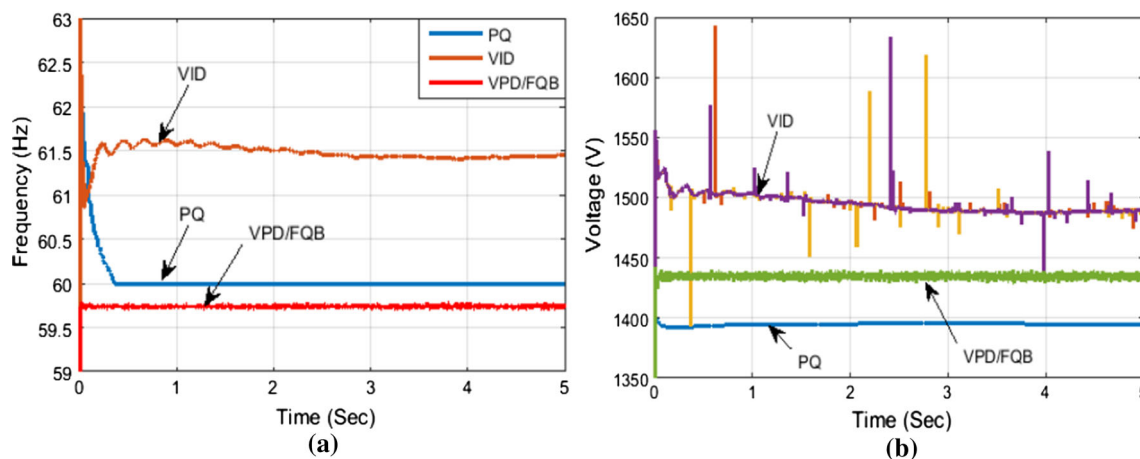


Fig. 3 **a** Frequency response of inverter-1 and **b** control voltage response of inverter-1

pared to 0.05 s for the conventional VID. Finally, real power is settled down at 172.3 KW in 0.9 s in case of conventional VPD/FQB, whereas it takes around 3 s to achieve quasi settled state, i.e. between 155 and 159 KW for the conventional VID scheme. However, for conventional PQ drooping scheme, the inverter response is very sluggish and it results to deliver only 142 KW of real power after 5 s. The delivered reactive power by the inverter-1 for the aforesaid three conventional drooping schemes is illustrated in Fig. 2b. The peak overshoot of reactive power in case of conventional VPD/FQB is 95.23 KVAR, whereas for conventional VID and PQ drooping, it is only 68.4 and 87.05 KVAR, respectively. The rise time of reactive power is 0.037 s in case of conventional VPD/FQB as compared to 0.42 s for conventional PQ drooping scheme and more than 3.5 s for conventional VID scheme. The dynamic frequency response and smooth response of the control voltage of the inverter-1 in case of the conventional VPD/FQB scheme is also comparatively better than the other two aforementioned conventional drooping schemes. The above comparisons justify the robust performance and effectiveness of the conventional VPD/FQB scheme as compared to conventional VID and conventional PQ drooping scheme in terms of improved dynamic response, less settling and rise time, and better efficiency. This performance of VPD/FQB scheme can be further enhanced in power sharing by integrating through designing appropriate control based on this approach. Figure 3a, b depicts the frequency response and control voltage response of inverter-1, respectively.

5 Proposed scheme

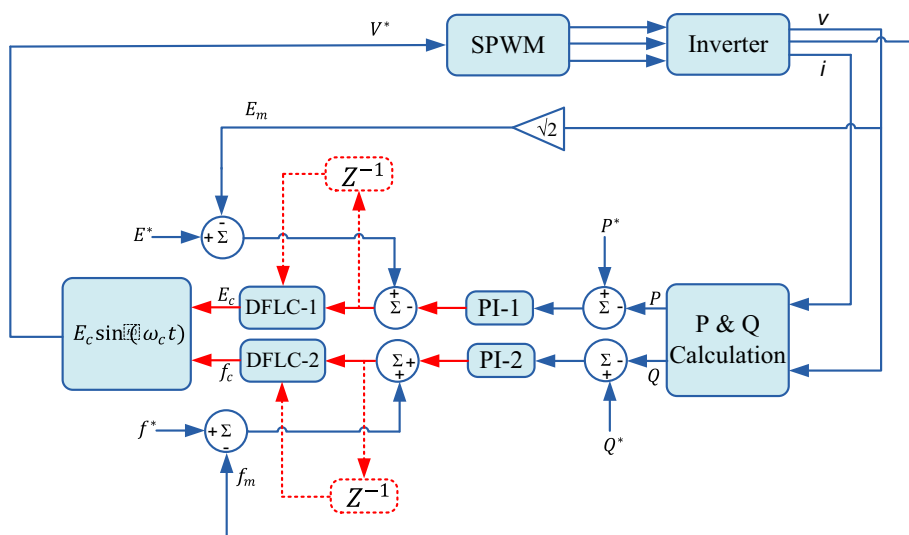
As seen in Sect. 4, conventional VPD/FQB scheme shows the finest result out of the three conventional schemes compared for the low-voltage feeder microgrid system. But in

order to further enhance the effectiveness and robustness of the VPD/FQB controller in terms of the load handling capacity, the dynamic response in transients, the settling time of the system, and the superior load sharing, the dynamic fuzzy logic controller (DFLC) is proposed in this work for the conventional VPD/FQB scheme.

5.1 Implementation of dynamic fuzzy logic controller (DFLC) in VPD/FQB scheme

Controlling a nonlinear system through a linear controller as proportional (P) or proportional–integral (PI) controller is difficult in the wider range of control and nonlinearity [22]. However, in respect to robustness and nonlinearity, the conventional FLC is an enhanced controller than the conventional P or PI controller [23]. Sometimes, conventional FLC may not provide satisfactory outcome due to the complexity and multivariable state of the power system. It has been found that in case of VFD/FQB scheme, the modest discrepancies of frequency or voltage of the VSI might be unsafe for the system. Deviation from the very precise value of frequency hampers appropriate power sharing, principally reactive power sharing. So to overcome these issues, dynamic fuzzy logic controller (DFLC) is anticipated with the VPD/FQB scheme. Figure 4 illustrates the strategies of VPD/FQB with DFCLC. For the controlling aspect of the inverter, only the local parameters like inverter voltage, ‘ V ’, inverter current, ‘ i ’, and inverter frequency ‘ f ’ are measured. From that measured parameters, real power P and reactive power Q are calculated. Calculated P and Q are compared to the reference real power P^* and reference reactive power Q^* , respectively, to generate error signals, which are then fed to PI controllers. For the DFCLC-1, the difference between reference E (E^*) and measured E (E_m) is compared to the output of the PI-1 controller to generate the error signal which is again fed to the DFCLC-1. Similarly, the DFCLC-2 difference

Fig. 4 Control strategies of VPD/FQB with DFCL



between reference f (f^*) and measured f (f_m) is compared to the output of the PI-2 controller to generate the error signal which is again fed to the DFCL-2. The rate of change of errors with respect to time is also used as a second set of inputs for both the DFCLs, control voltage (E_c) and control frequency (f_c), generate the signal $E_c \sin(\omega_c t)$, which is then fed to SPWM as control signal.

5.2 Modelling of DFCL

The proposed DFCL controller is a nonlinear controller and provides more robustness in control scheme compared to the conventional FLC and PI controller. In this proposed control scheme, a Mamdani-type fuzzy inference system (FIS) is taken into consideration for the DFCL. The different steps involved in DFCL like fuzzification, fuzzy rule base, fuzzy inference system, and defuzzification are briefly discussed below.

5.2.1 Fuzzification

In general, there are two inputs that are taken for the purpose of fuzzification, first is the error $e(n)$, i.e. error in reactive power ΔQ , and second is the rate of change of error $r(n)$, i.e. $\frac{d}{dt}(\Delta Q)$. Mathematically in Eqs. (1) and (2), $e(n)$ and $r(n)$ are expressed as follows [24]:

$$e(t) = s(t) - y(t) \tag{1}$$

$$r(t) = e(t) - e(t - 1) = y(t - 1) - y(t) \tag{2}$$

where $s(t)$ represents the system desired value and $y(t)$ is the output of the controller.

Two fuzzy sets are defined to fuzzify the inputs $e(t)$ and $r(t)$. Fuzzy sets are generally expressed by various types of membership functions (MF), namely as trapezoidal, bell-shaped, and triangular [25]. In this case, triangular MF is considered. Here the linguistic variables assigned to this DFCL are negative large (NL), negative medium (NM), negative small (NS), zero (ZE), positive small (PS), positive medium (PM), and positive large (PL). One MF function for $e(n)$ and one MF for $r(n)$ are shown in Figs. 5 and 6, respectively.

5.2.2 Rule base

Through fuzzified input, the rule base is originated [26]. Fuzzy statements ‘IF’ and ‘THEN’ are combined through operator ‘AND’. Table 1 depicts the DFCL 49 rules. Figures 7 and 8 show the three-dimensional surface viewer and rule viewer, respectively.

5.2.3 Fuzzy inference

After generation of membership functions from the fuzzified inputs, they are implicated through fuzzy operator ‘AND’ to produce output MF, $y(n)$. The fuzzified output is shown in Fig. 9, where $y(n)$ is the output frequency, f .

5.2.4 Defuzzification

The proposed dynamic fuzzy logic controller uses centre of area (COA) method to determine the final de-fuzzified output. In this case, the de-fuzzified output is the control frequency of the inverter f_c , as given in Eq. (3).

Fig. 5 Membership function of $e(n)$

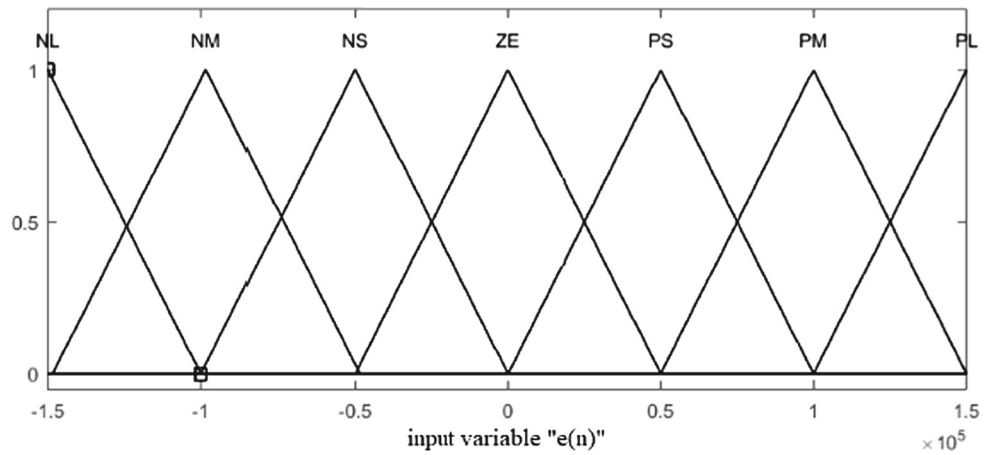


Fig. 6 Membership function of $r(n)$

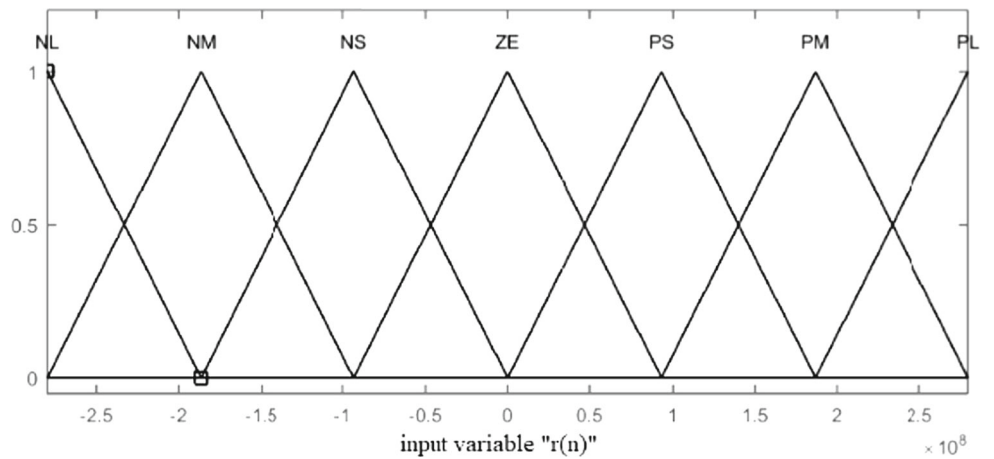


Table 1 Rule base used for proposed DFLLC

		$e(n)$						
		NL	NM	NS	ZE	PS	PM	PL
$r(n)$	NL	PU	PU	PL	PM	PM	PS	ZE
	NM	PU	PL	PL	PM	PS	ZE	NS
	NS	PL	PL	PM	PS	ZE	NS	NM
	ZE	PL	PM	PS	ZE	NS	NM	NL
	PS	PM	PS	ZE	ZE	NM	NL	NL
	PM	PS	ZE	NS	ZE	NL	NL	NU
	PL	ZE	NS	NM	NS	NL	NL	NU

$$f_c = \frac{\sum_{i=1}^m \mu(f_{c_i}) \cdot f_{c_i}}{\sum_{i=1}^m \mu(f_{c_i})} \tag{3}$$

6 Simulation results and analysis

To evaluate the performance of the proposed control scheme, the islanded microgrid study system is simulated in MATLAB/Simulink environment as depicted in Fig. 1. The

parameters of the systems are cited in “Appendix”. The model comprises of two DG units and two loads through transmission line offering wire impedances connected to the PCC. Both the interfacing SPWM inverters involve control strategies as illustrated in Sect. 3. Two LC low-pass filters are placed between the IGBT bridge output and the DG feeder. The real and the reactive power are calculated by measuring the DG line current and filter capacitor voltage. The two linear isolation transformers (DIYg) are used to step

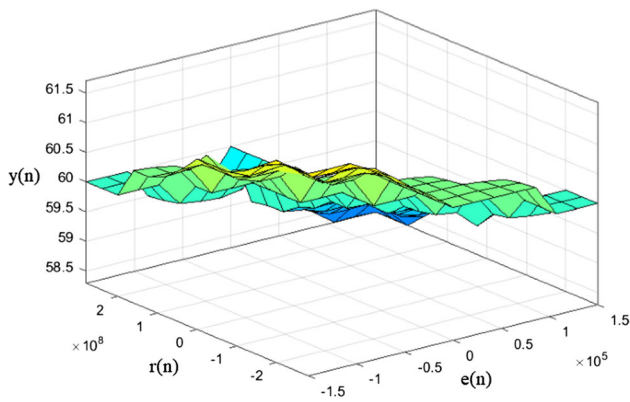
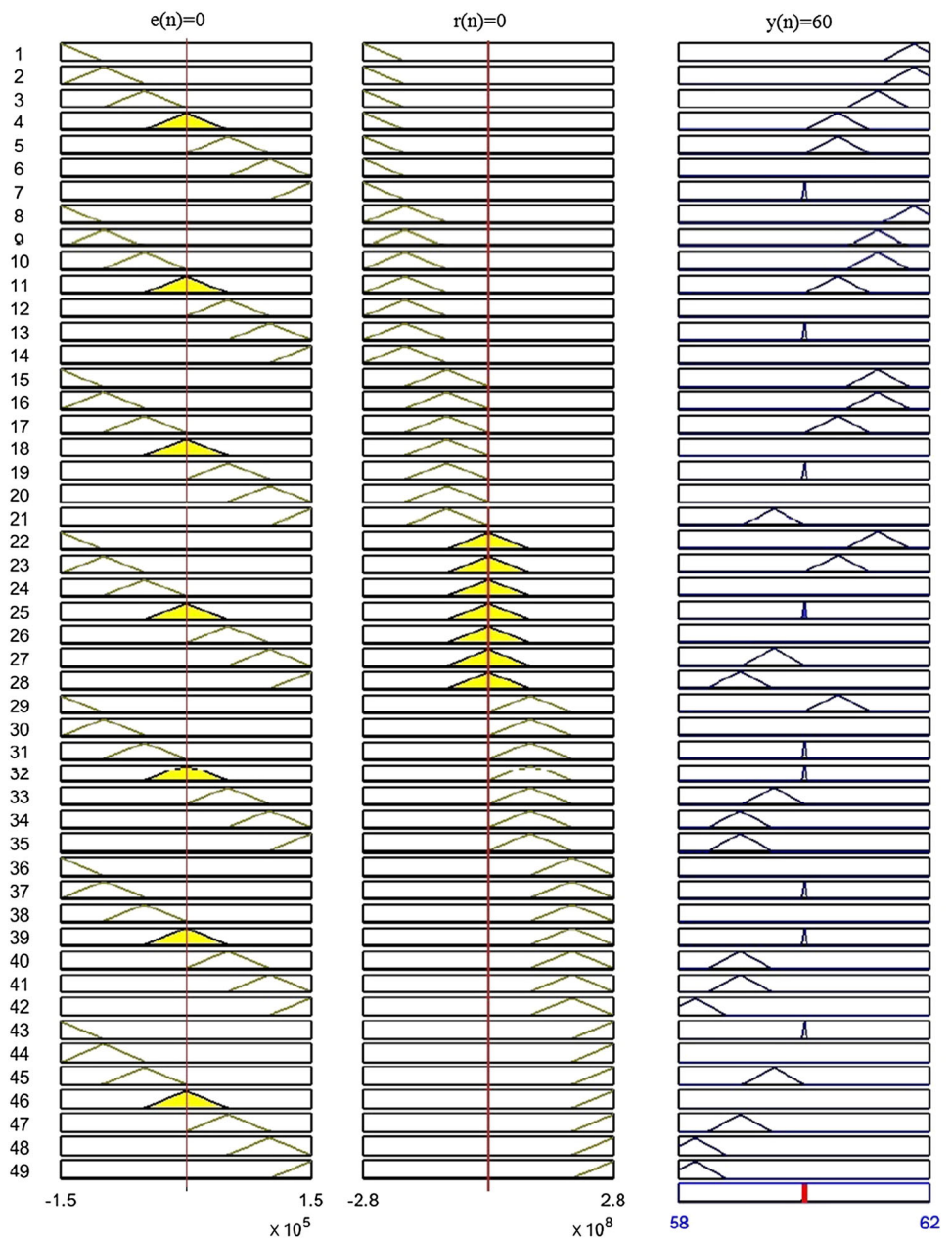


Fig. 7 3D surface view

Fig. 8 Rule view of 49 control rules



down the output voltage of the inverter in order to match the load requirement. The T-type transmission line is considered, which consists of series inductance, resistance, and ground capacitance.

6.1 Case-I: Performance analysis of islanded microgrid power generating system with nonlinear load switching

Figures 10, 11, 12, and 13 show real and reactive power sharing by DG1 and DG2, the frequency response of inverter-1 and control voltage response of inverter-1, load current, and load voltage, the percentage of error in power tracking, and percentage of increment of power delivery, respectively, as

Fig. 9 Output membership function of $y(n)$

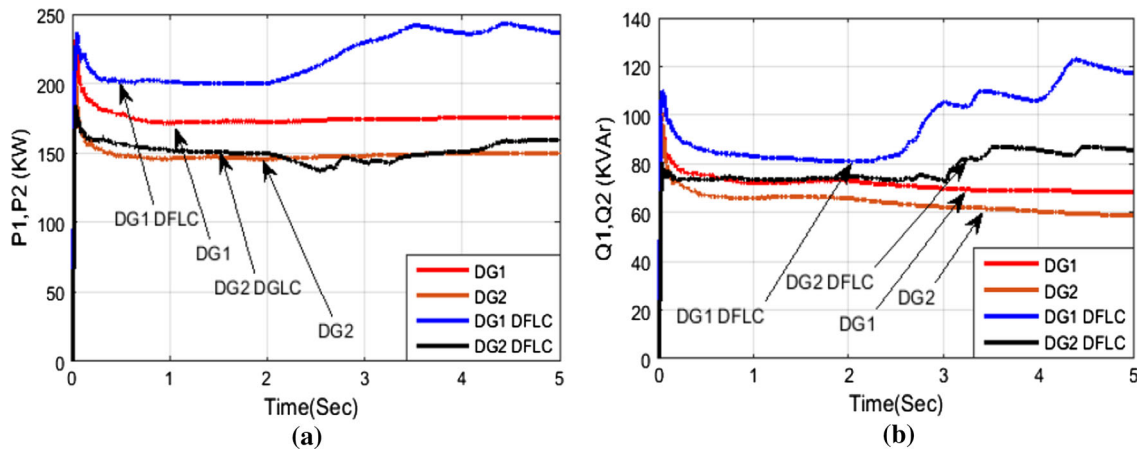
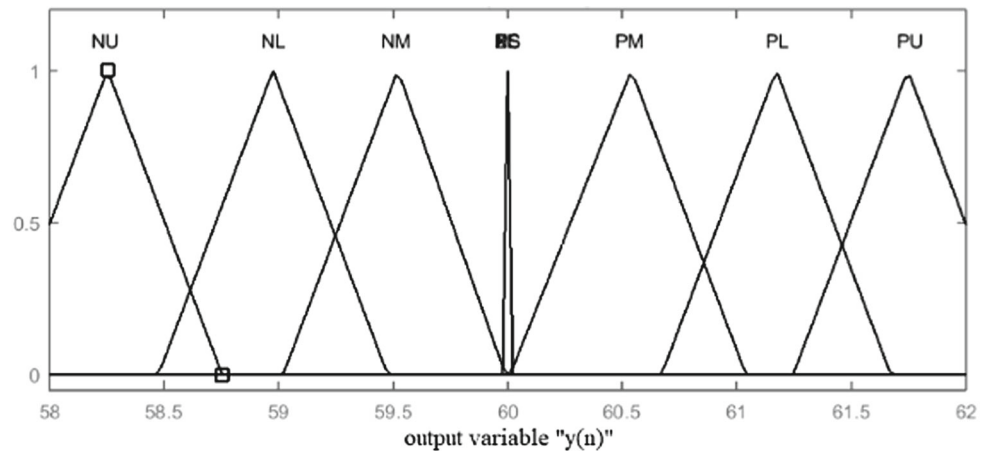


Fig. 10 **a** Real power sharing by DG1 and DG2 and **b** reactive power sharing by DG1 and DG2

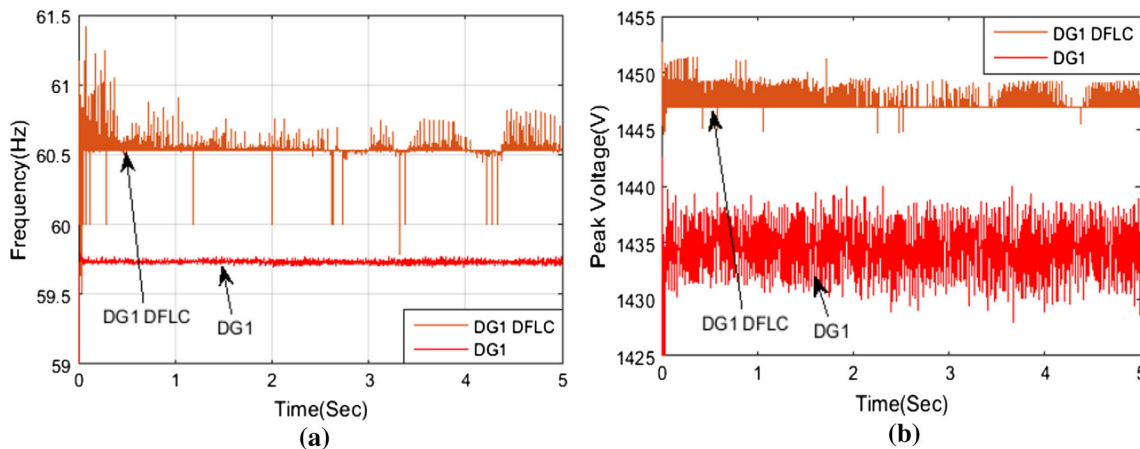


Fig. 11 **a** Frequency response of inverter-1, and **b** control voltage response of inverter-1

subjected to nonlinear load switching. At $t = 2$ s, a nonlinear load (three-phase thyristor converter) is switched on. On account of the nonlinearity of the load, the islanded power generating microgrid system becomes unstable. To compen-

sate the aforesaid issue, a novel technique, DFLC-based VPD/FQB, is proposed in this paper. The peak overshoot of real power and reactive power obtained by implementing DFLC is 4.9 and 15.8%, respectively, greater than that

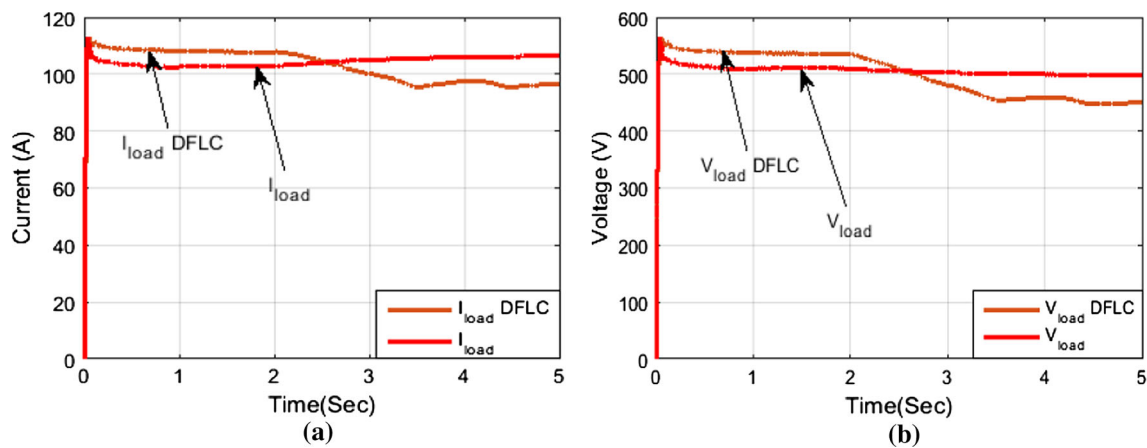


Fig. 12 a Load current and b load voltage

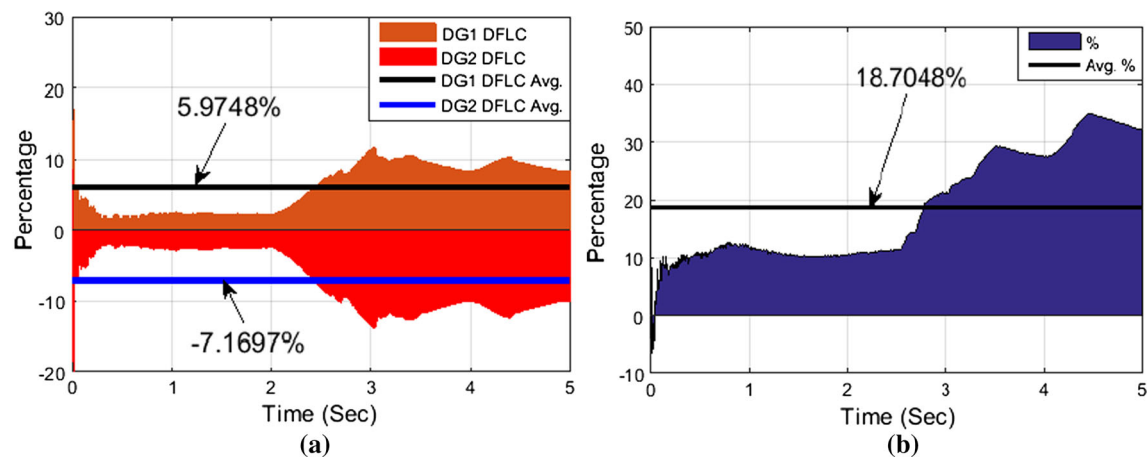


Fig. 13 a Percentage of error in power tracking and b percentage of increment of power delivery

obtained without DFLC. The active power of the system with VPD/FQB has the settling time of 0.7 s, whereas it is only 0.3 s (approximately half) in case of the proposed DFLC controller as shown in Fig. 10a, b and illustrates that the rise time of the reactive power in case of conventional VPD/FQB is 0.04 s, whereas it is 0.03 s for the DFLC. It can be also seen that DFLC has a peak frequency of 61.4 Hz compared to 59.78 Hz in use of VPD/FQB as depicted in Fig. 11a. The load voltage characteristics have a settling time of 0.07 s for VPD/FQB, whereas it is comparatively less, i.e. 0.05 s in case of DFLC as illustrated in Fig. 12b. The increment of mean average power delivery by proposed DFLC-based VPD/FQB over conventional VPD/FQB is 18.7048% as illustrated in Fig. 13b. Apart from that, inverter-1 and inverter-2 show only 5.9748 and -7.1697% of error in power tracking, respectively, as shown in Fig. 13a. The above comparisons justify the enhanced performance and effectiveness of the proposed dynamic FLC-based VPD/FQB technique as compared to conventional VPD/FQB in terms of greater speed in computation, improved dynamic response, less settling and rise time, and better efficiency.

6.2 Case-II: Performance analysis of islanded microgrid power generating system with constant real power and variable (switched at $t = 2$ s) reactive power

Figures 14, 15, 16, and 17 illustrate real and reactive power sharing by DG1 and DG2, the frequency response of inverter-1 and control voltage response of inverter-1, load current, and load voltage, the percentage of error in power tracking, and percentage of increment of power delivery, respectively, as subjected to constant real power and variable reactive power. At $t = 2$ s, a reactive load is switched on. A comparison is executed between conventional VPD/FQB and proposed DFLC-based VPD/FQB for this case. Figure 14a illustrates that the peak overshoot of real power is 3.03% and the peak overshoot of reactive power is 17.89% more for the proposed DFLC-based VPD/FQB over the conventional VPD/FQB. Settling time for the active power is only 0.25 s in case of the proposed scheme, whereas it is 0.7 s for the conventional one as illustrated in Fig. 14a.

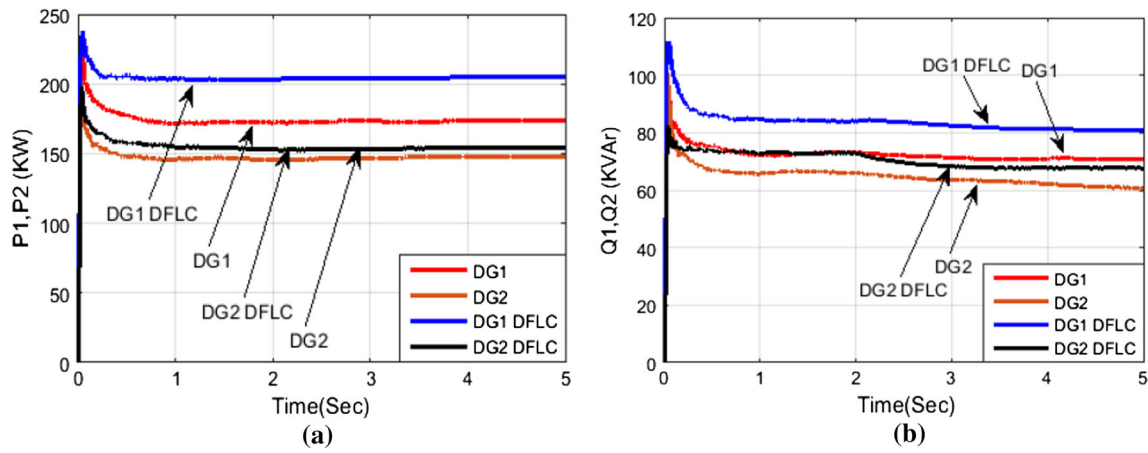


Fig. 14 a Real power sharing by DG1 and DG2 and b reactive power sharing by DG1 and DG2

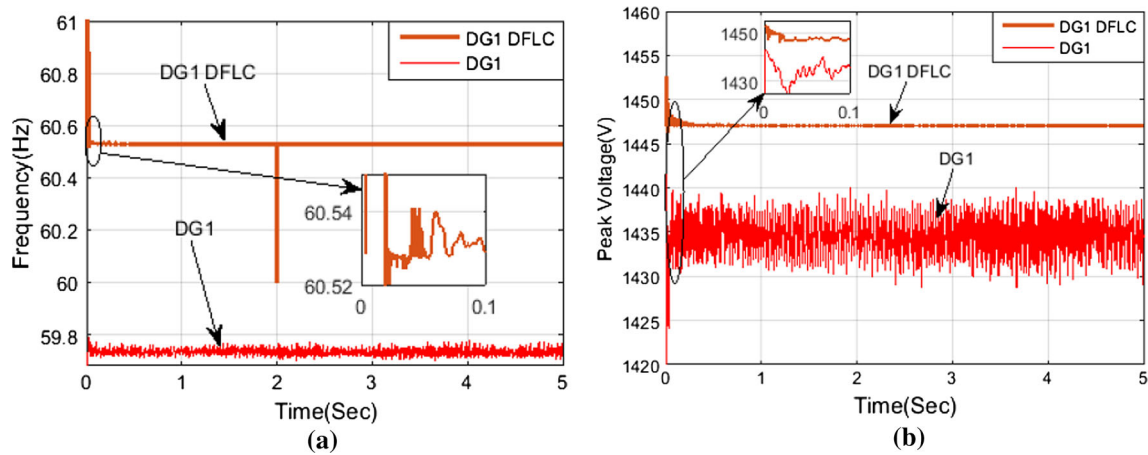


Fig. 15 a Frequency response of inverter-1 and b control voltage response of inverter-1

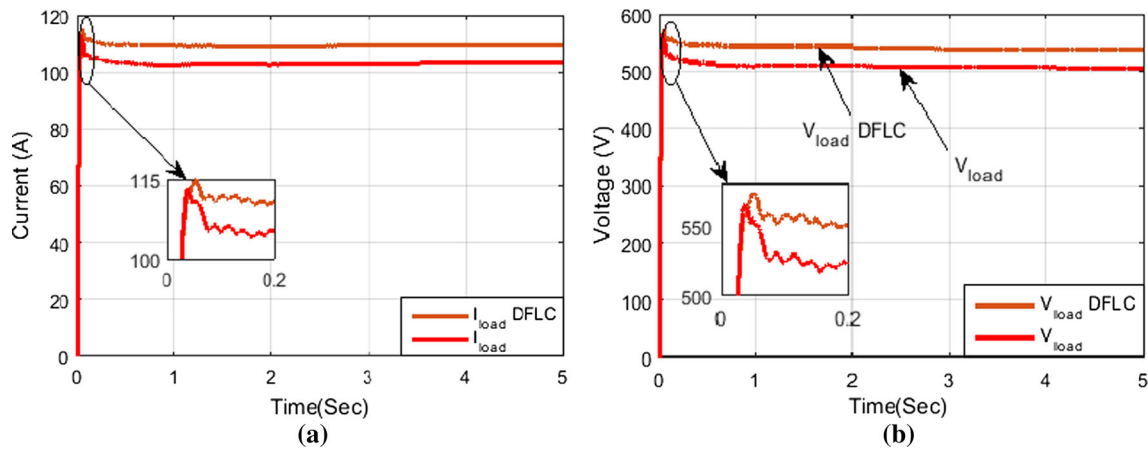


Fig. 16 a Load current and b load voltage

Again from Fig. 14a, it is clear that rise time of real power is only 0.029 s for the proposed DFLC-based scheme, whereas it is 0.038 s for the conventional VPD/FQB scheme. Figure 14b illustrates that the peak overshoot of reactive

power is 17.89% more for the proposed scheme over the conventional scheme. The settling time of reactive power is 0.27 s and 0.38 s for the proposed scheme and conventional scheme, respectively, as depicted in Fig. 14b. It can be also

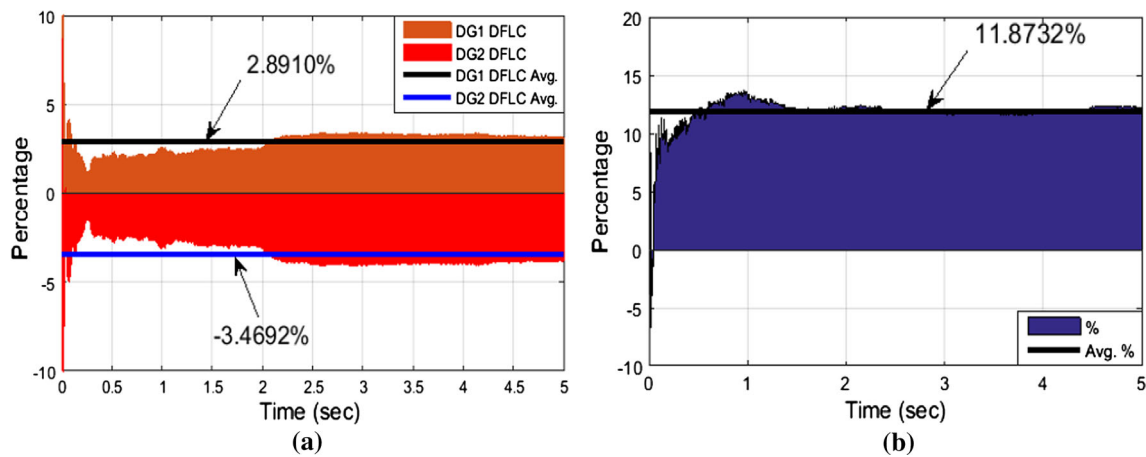


Fig. 17 a Percentage of error in power tracking and b percentage of increment of power delivery

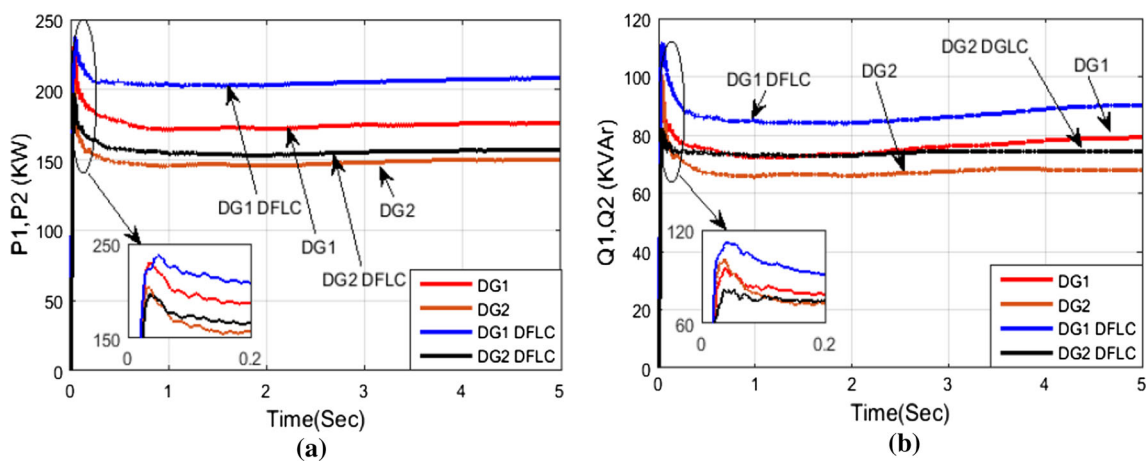


Fig. 18 a Real power sharing by DG1 and DG2 and b reactive power sharing by DG1 and DG2

seen that the DFCL has a peak frequency of 61 Hz whereas VPD/FQB has 59.78 Hz as shown in Fig. 15a. Figure 16 gives the peak overshoot of load current and load voltage as 1.77 and 1.42%, respectively, more in the proposed scheme. Also for the proposed DFCL-based VDD/FQB scheme, the overall increment of power is 11.8732% more over the conventional, which shows only 2.8910% error by inverter-1 and -3.4692% error by inverter-2 in power tracking as illustrated in Fig. 17. The above comparisons justify the superiority of proposed DFCL-based VPD/FQB scheme.

6.3 Case-III: Performance analysis of islanded microgrid power generating system with constant reactive power and variable (switched at $t = 2$ s) real power

Figures 18, 19, 20, and 21 illustrate real and reactive power sharing by DG1 and DG2, the frequency response of inverter-1 and control voltage response of inverter-1, load current, and load voltage, the percentage of error in power tracking, and

percentage of increment of power delivery, respectively, as subjected to constant reactive power and variable real power. At $t = 2$ s, a purely resistive load is switched on.

A comparison is executed between conventional VPD/FQB and proposed DFCL-based VPD/FQB for this case. The peak overshoot of real power and reactive power obtained by implementing DFCL is 4.34 and 17.89%, respectively, greater than that obtained without DFCL. The active power of the system with VPD/FQB has the settling time of 0.9 s, whereas it is only 0.24 s in case of the proposed DFCL controller as shown in Fig. 18a. Settling time for the reactive power is only 0.36 s in case of the proposed scheme whereas it is 0.57 s for the conventional one as illustrated in Fig. 18b. Peak overshoot of reactive power is 17.89% more by the proposed DFCL-based VPD/FQB over the conventional VPD/FQB. It can be also seen that DFCL has a peak frequency of 61.172 Hz compared to 59.8 Hz in case as illustrated in Fig. 19a. Here for the proposed scheme, the peak overshoot of load current and load voltage is 1.59% more than the conventional VPD/FQB, as implicated in Fig. 20.

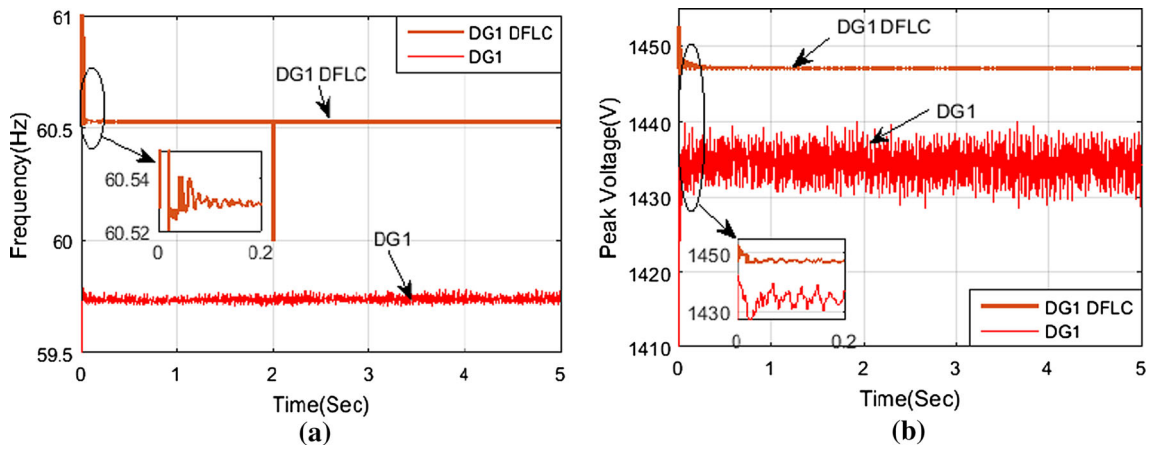


Fig. 19 a Frequency response of inverter-1 and b control voltage response of inverter-1

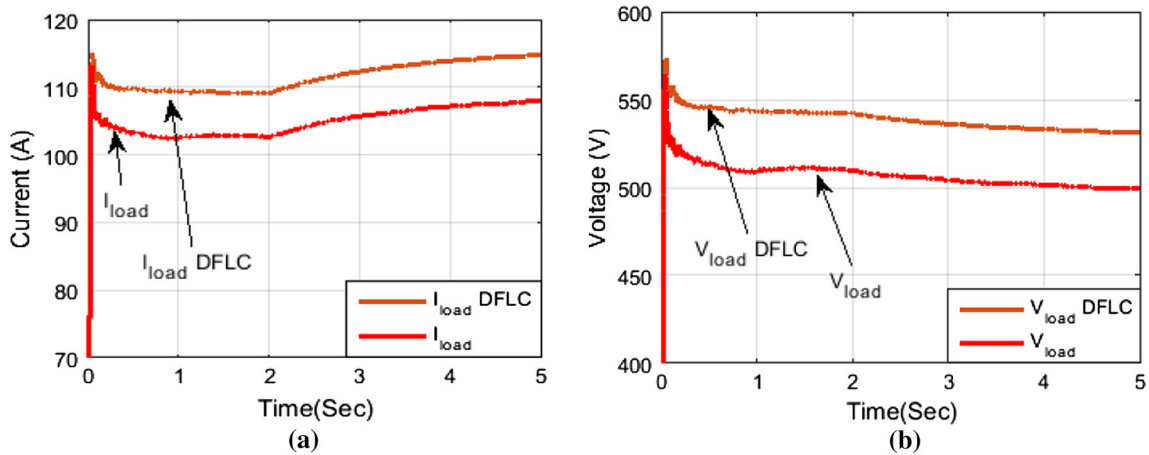


Fig. 20 a Load current and b load voltage

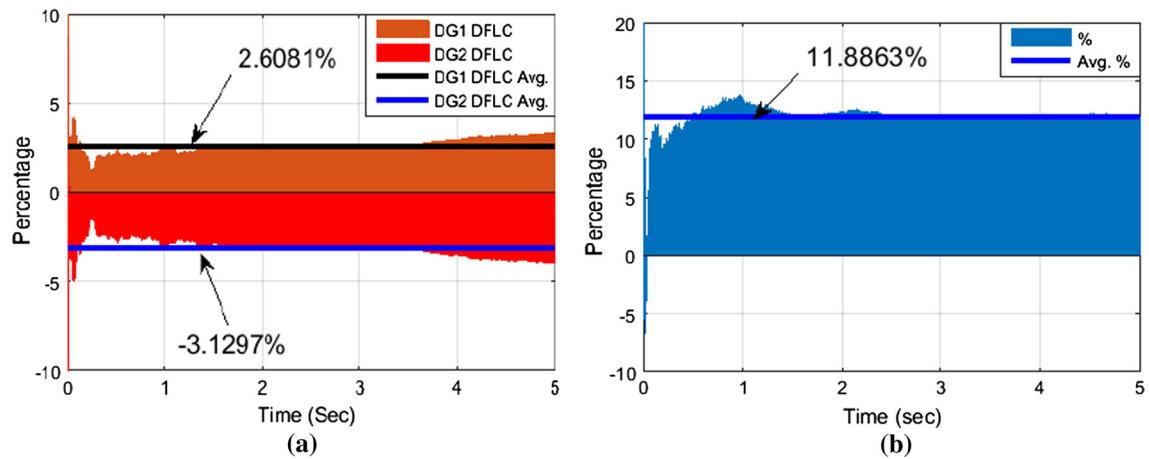


Fig. 21 a Percentage of error in power tracking and b percentage of increment of power delivery

The increment of mean average power delivered by proposed DFLC-based VPD/FQB over conventional VPD/FQB is 11.8863% as shown in Fig. 21b. Inverter-1 and inverter-2 show only 2.6081 and -3.1297% of error in power tracking, respectively, as depicted in Fig. 21a. The above comparisons

justify the enhanced performance and effectiveness of the proposed dynamic FLC-based VPD/FQB technique as compared to conventional VPD/FQB in terms of greater speed in computation, improved dynamic response, less settling and rise time, and better efficiency.

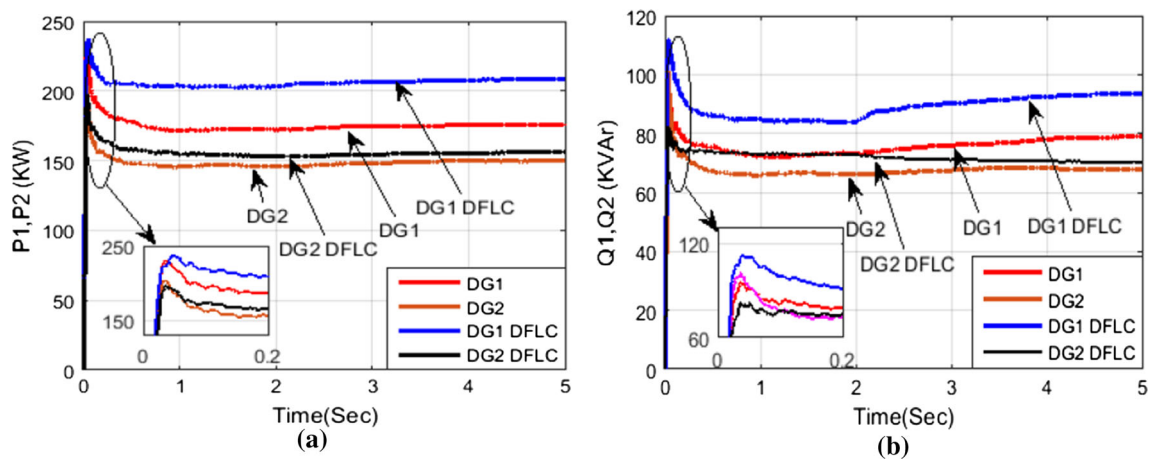


Fig. 22 a Real power sharing by DG1 and DG2 and b reactive power sharing by DG1 and DG2

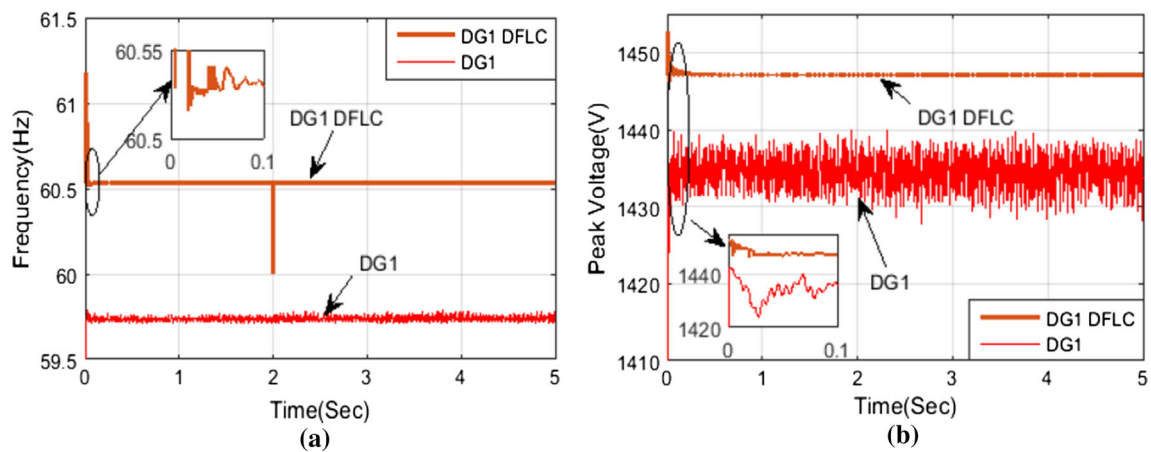


Fig. 23 a Frequency response of inverter-1 and b control voltage response of inverter-1

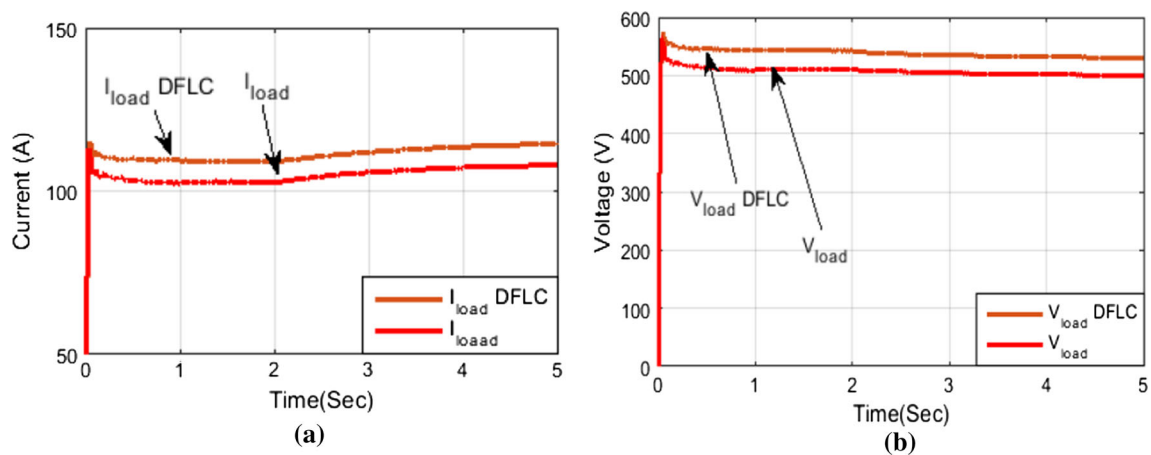


Fig. 24 a Load current and b load voltage

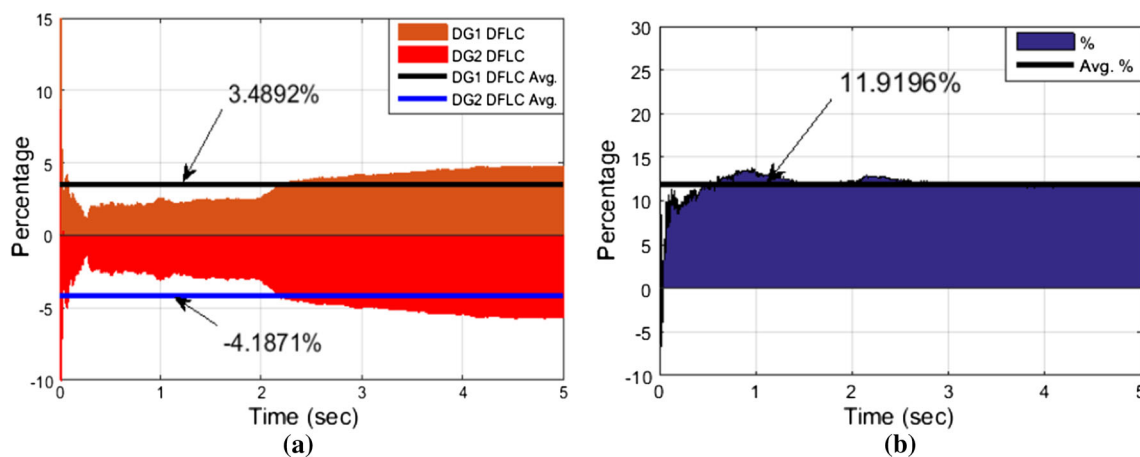


Fig. 25 a Percentage of error in power tracking and b percentage of increment of power delivery

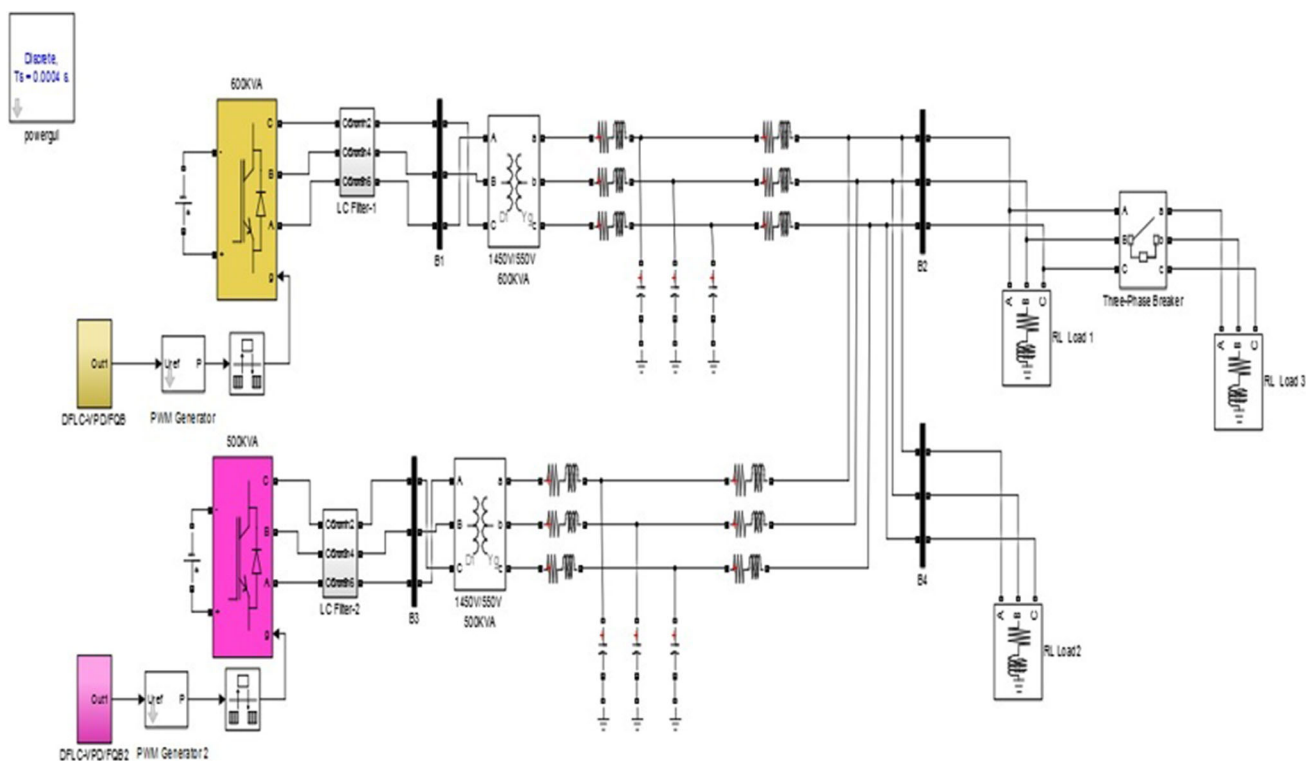


Fig. 26 MATLAB/Simulink model of DFLC-based VPD/FQB

6.4 Case-IV: Performance analysis of islanded microgrid power generating system with unsymmetrical load switching (at $t = 2$ s)

Figures 22, 23, 24, and 25 show real and reactive power sharing by DG1 and DG2, frequency response of inverter-1 and control voltage response of inverter-1, load current, and load voltage, the percentage of error in power tracking, and the percentage of increment of power delivery, respec-

tively, as subjected to the unsymmetrical load switching. At $t = 2$ s, an unsymmetrical load is switched on. On account of the asymmetry of the load, the islanded power generating microgrid system becomes unstable. To compensate the aforementioned issue, a novel control scheme, DFLC-based VPD/FQB is employed. Figure 22a shows that the peak overshoot of real power is 2.94% and the peak overshoot of reactive power is 17.28% more by the proposed DFLC-based VPD/FQB over the conventional VPD/FQB.

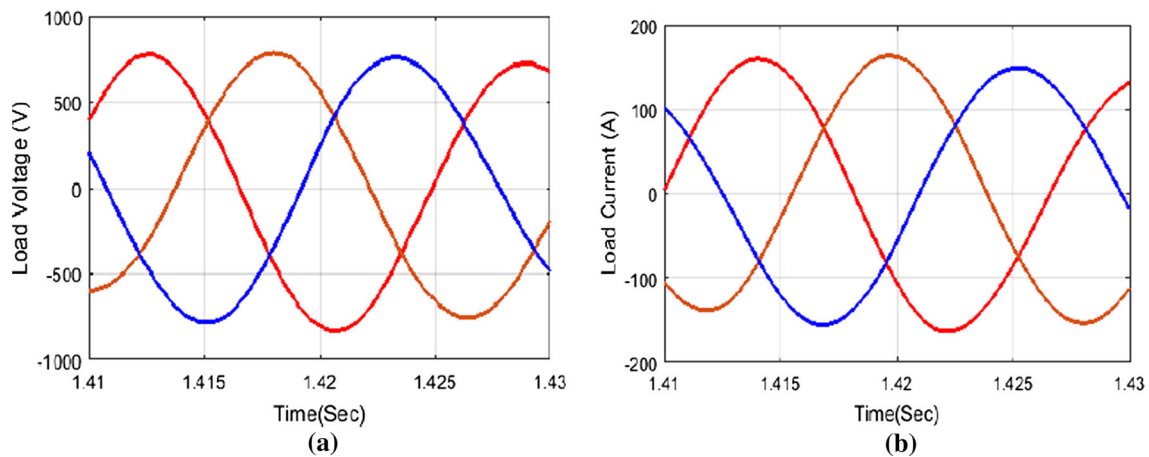


Fig. 27 **a** Load voltage and **b** load current

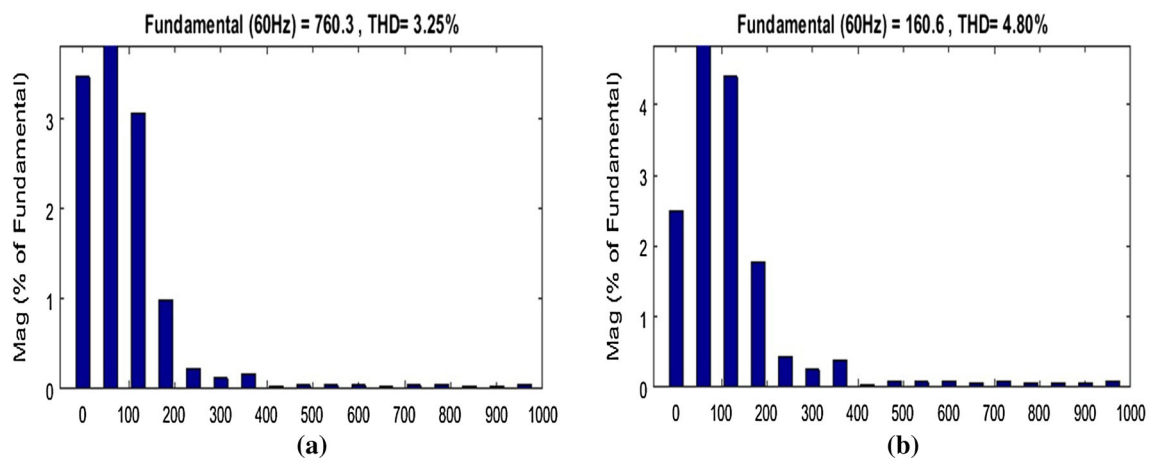


Fig. 28 **a** FFT analysis of load voltage and **b** FFT analysis of load current

Settling time for the active power is only 0.3 s in case of the proposed scheme, whereas it is 0.9 s for the conventional one as illustrated in Fig. 22a. Figure 22b shows the settling time of reactive power is 1 s for the case of proposed scheme, whereas for the conventional scheme it is in queasy settled condition. It can also be observed in Fig. 23a that the DFCLC has a peak frequency of 61.172 Hz, whereas VPD/FQB has 59.786 Hz. For the proposed DFCLC-based VPD/FQB scheme, the control voltage of inverter-1 is offering a smooth dynamic response as depicted in Fig. 23b. For this case, peak overshoot of load current and load voltage is achieved as 1.59 and 1.55%, respectively, more through the proposed scheme, which is shown in Fig. 24. Through the proposed DFCLC-based VPD/FQB scheme, the overall increment of power is 11.9196% more than the conventional, which shows only 3.4892% error by inverter-1 and -4.1871% errors by inverter-2 in power tracking, respectively, as illustrated in Fig. 25. From this above comparison, it is justified that proposed DFCLC-based VPD/FQB poses superiority in terms of enhanced dynamic response and less computation time.

6.5 Case-V: Simulink model with THD calculation and FFT analysis

For the complete perception, a systematically designed model in MATLAB/Simulink software for the proposed DFCLC-based VPD/FQB scheme is shown in Fig. 26. Figure 27a, b shows the load voltage and load current. The fast Fourier transform (FFT) analysis of load voltage and load current is shown in Fig. 28a, b, respectively. The total harmonic distortion (THD) for the maximum frequency of 1000 Hz is found out to be 3.25% for the load voltage and 4.80% for the load current, respectively. For both the cases, the values lie well within the IEEE prescribed limits.

7 Conclusion

In this paper, two parallel-connected micro-sources are integrated through interfacing inverters, and the islanded mode of operation has been modelled and simulated using MATLAB/Simulink. Three conventional drooping schemes, namely PQ drooping, virtual impedance drooping, and

VPD/FQB, are considered to control the interfacing inverters for proper load sharing, and the comparative simulated results are presented to evaluate their efficiency and robustness in respect to settling time, rise time, peak overshoot, stability, and dynamic response. In order to further enhance the controllability and performance of VPD/FQB, the best-suited conventional drooping scheme among the three conventional approaches, a dynamic fuzzy logic controller, is proposed and implemented. In this proposed control strategy, fuzzy input parameters are dynamically tuned by PI controllers and by so the concept of constant fuzzy parameters is avoided. The proposed DFCLC-based VPD/FQB is compared with respect to conventional VPD/FQB subjected to critical load conditions to verify the efficiency, system response time, settling time, robustness, and reliability. The comparative demonstrations validate the effectiveness of the proposed scheme in terms of efficiency, robustness, and reliability. THD through FFT analysis of the load voltage and current is also carried out to ensure the system harmonics limit lies within the prescribed IEEE standard.

Appendix

The parameters of the studied system, shown in Fig. 1, are given below.

DC Source (V_{dc}): 2500 V. *Inverter*: inverter-1 rating = 600 KVA; inverter-2 rating = 500 KVA; *Inverter filter* : $L_f = 5$ mH; $C_f = 300$ μ F. *Transformer*: nominal power-1 = 600 KVA; nominal power-2 = 500 KVA; nominal frequency = 60 Hz; $V_{1\text{rms}}(\text{Ph} - \text{Ph}) = 1450$ V; $R_1(\text{PU}) = 0.02/25$; $L_1(\text{PU}) = 0.02$; $V_{2\text{rms}}(\text{Ph} - \text{Ph}) = 550$ V; $R_2(\text{PU}) = 0.02/25$; $L_2(\text{PU}) = 0.02$. *Transmission line*: $R_T = 1$ Ω/km ; $L_T = 1$ Ω/km ; $C_T = 90$ μ F. *Load*: $P_{\text{constant}} = 80$ KW; $Q_{\text{constant}} = 10$ KVAR; $I_{\text{nonlinear}}$ (rms line current) = 15 = A; $P_{(1-\text{Ph})} = 10$ KW; $Q_{\text{Switched}} = 10$ KVAR.

References

- Moslehi K, Kumar R (2010) A reliability perspective of the smart grid. *IEEE Trans Smart Grid* 1(1):57–64
- Lasseter RH (2002) Microgrids. In: *Proceedings of IEEE power engineering society winter meeting*, pp 305–308
- Rocabert J, Luna A, Blaabjerg F, Rodriguez P (2012) Control of power converters in AC microgrids. *IEEE Trans Power Electron* 27(11):4734–4739
- Molderink A, Bakker V, Bosman MGC, Hurink JL, Smit GJM (2010) Management and control of domestic smart grid technology. *IEEE Trans Smart Grid* 1(2):109–119
- Blaabjerg F, Teodorescu R, Liserre M, Timbus AV (2006) Overview of control and grid synchronization for distributed power generation systems. *IEEE Trans Ind Electron* 53(5):1398–1409
- Yu X, Khambadkone AM, Wang H (2010) Control of parallel-connected power converters for low-voltage microgrid—part I: a hybrid control architecture. *IEEE Trans Power Electron* 25(12):2962–2970
- Simpson-Porco JW, Dörfler F, Bullo F (2017) Voltage stabilization in microgrids via quadratic droop control. *IEEE Trans Autom Control* 62(3):1239–1253
- He J, Li YW (2012) An enhanced microgrid load demand sharing strategy. *IEEE Trans Power Electron* 27(9):3984–3995
- Pogaku N, Prodanovic M, Green TC (2007) Modeling, analysis and testing of autonomous operation of an inverter-based microgrid. *IEEE Trans Power Electron* 22(2):613–625
- Sao CK, Lehn PW (2008) Control and power management of converter fed microgrids. *IEEE Trans Power Syst* 23(3):1088–1098
- Chandorkar MC, Divan DM, Adapa R (1993) Control of parallel connected inverters in standalone ac supply systems. *IEEE Trans Ind Appl* 29(1):136–143
- Debrabandere K, Bolsens B, Van den Keybus J, Woyte A, Driesen J, Belmans R (2007) A voltage and frequency droop control method for parallel inverters. *IEEE Trans Power Electron* 22(4):1107–1115
- Guerrero JM, GarcíadeVicuna L, Matas J (2005) Output impedance design of parallel-connected UPS inverters with wireless load-sharing control. *IEEE Trans Ind Electron* 52(4):1126–1135
- Yao W, Chen M, Matas J (2011) Design and analysis of the droop control method for parallel inverters considering the impact of the complex impedance on the power sharing. *IEEE Trans Ind Electron* 58(2):576–588
- Guerrero JM, Vasquez JC, Matas J (2011) Hierarchical control of droop-controlled AC and DC microgrids—a general approach toward standardization. *IEEE Trans Ind Electron* 58(1):158–172
- Guerrero JM, Loh P, Chandorkar M (2013) Advanced control architectures for intelligent microgrids—part I: decentralized and hierarchical control. *IEEE Trans Ind Electron* 60(4):1254–1262
- Sundarabalan CK, Selvi K (2017) Real coded GA optimized fuzzy logic controlled PEMFC based dynamic voltage restorer for reparation of voltage disturbances in distribution system. *Int J Hydrog Energy* 42(1):603–613
- Spiro RJ, Bruce BC, Brewer WF (eds) (2017) *Theoretical issues in reading comprehension: perspectives from cognitive psychology, linguistics, artificial intelligence and education*, vol 11. Routledge, London
- Blaabjerg F, Stig M-N (1995) Power losses in PWM-VSI inverter using NPT or PT IGBT devices. *IEEE Trans Power Electron* 10(3):358–367
- Han H et al (2016) Review of power sharing control strategies for islanding operation of AC microgrids. *IEEE Trans Smart Grid* 7(1):200–215
- Han Y et al (2017) Control strategies for islanded microgrid using enhanced hierarchical control structure with multiple current-loop damping schemes. *IEEE Trans Smart Grid* 8(3):1139–1153
- O’Dwyer A (2009) *Handbook of PI and PID controller tuning rules*, vol 57. Imperial College Press, London
- Lee C-C (1990) Fuzzy logic in control systems: fuzzy logic controller. I. *IEEE Trans Syst Man Cybern* 20(2):404–418
- Timothy RJ (2004) *Fuzzy logic with engineering applications*, 2nd edn. Wiley, London
- Miyatake M, Toriumi F, Endo T, Fujii N (2007) A novel MPPT controlling several converters connected to PV arrays with PSO technique. In: *Proceedings of power electronics application European conference 2007*, pp 1–10
- Sri Vidhya D, Venkatesan T, Kanagaraj N (2017) Fuzzy logic controller for variable boost function in quasi Z source indirect matrix converter during voltage sag condition. *Int J Fuzzy Syst* 19(4):1093–1103

Publisher’s Note Springer Nature remains neutral with regard to jurisdictional claims in published maps and institutional affiliations.